Available online at www.sciencedirect.com
SCIENCE DIRECT®
Journal of Nuclear Materials 340 (2005) 171–178
journal of nuclear materials
www.elsevier.com/locate/jnucmat

Electrical conductivity and non-stoichiometry in the (U,Gd)$O_{2\pm x}$ system

Jae Ho Yang *, Keon Sik Kim, Ki Won Kang, Kun Woo Song, Youn Ho Jung

Advanced LWR Fuel Development, Korea Atomic Energy Research Institute (KAERI), Deokjin-dong 150, Yuseong-gu, Daejeon-si 305-600, Republic of Korea

Received 16 July 2004; accepted 10 November 2004

Abstract

The isothermal electrical conductivity and oxygen potential of the (U,Gd)$O_{2\pm x}$ solid solution were measured in various oxygen partial pressure regions at 1200 °C and 1300 °C. The electrical conductivity gradually decreased with decreasing oxygen partial pressure even in the hypo-stoichiometric region. These findings were in contrast to the implication of a hypo-stoichiometry where the electrical conductivity is increased through the formation of oxygen vacancies. The ($U_{1-y}Gd_y$)$O_{2-y/2}$ was defined as a new stoichiometric composition to determine the relationship between the deviation of the oxygen composition from stoichiometry and oxygen partial pressure. The dependence of the new oxygen deviation, z in ($U_{1-y}Gd_y$)$O_{2-y/2+z}$, on the oxygen partial pressure corresponds to the dependence of the electrical conductivity, and thus a consistent defect structure model can be deduced from both the dependence curves. It suggests that the defect type is oxygen interstitial even below the oxygen composition of 2.

1. Introduction

Uranium dioxide can accommodate large amounts of excess oxygen atoms, with its cubic symmetry maintained [1–7]. Incorporated and displaced lattice oxygen atoms form defect aggregates called oxygen defect clusters. Various kinds of oxygen defect cluster models have been suggested. Among these, the Willis's ($2O_i^a 2V_O 2O_i^b$) defect cluster [1,7] and the cuboctahedral cluster [5,8–10] are commonly used for interpreting a defect cluster in the UO_{2+x} system. The oxygen defect structure and its ionization state in the UO_{2+x} system are often deduced from the dependence of the oxygen partial pressure, p_{O_2}, on the oxygen deviation from stoichiometry (x) and /or electrical conductivity (σ) [11–15]. The deviation (x) and the electrical conductivity (σ) have similar correlations with the oxygen partial pressure, i.e., $x \propto p_{O_2}^{1/\alpha}$ and $\sigma \propto p_{O_2}^{1/\beta}$, respectively. The α and β values convey some important information on the defect structure. Thus, the oxygen defect structure can be deduced from the α and β values by applying an appropriate defect model.

A mixture of UO_2 and neutron-absorbing lanthanide oxides (Ln_2O_3), which is in the form of ($U_{1-y}Ln_y$)O_2, is used to control the nuclear fission in nuclear reactors, together with UO_2 fuel [16–19]. A trivalent Ln^{3+} cation substitution leads to changes in the relationship between the oxygen-to-metal (O/M) ratio and oxygen partial pressure. The O/M ratios at all the oxygen partial pressures are decreased by the substitution of the Ln^{3+} cation. In the low oxygen partial pressure region [20,21],

* Corresponding author. Tel.: +82 42 868 2813; fax: +82 42 861 7340.
E-mail address: yangjh@kaeri.re.kr (J.H. Yang).

0022-3115/$ - see front matter © 2004 Elsevier B.V. All rights reserved.
doi:10.1016/j.jnucmat.2004.11.006

the metal-to-oxygen ratio becomes even smaller than 2.0, i.e. $(U_{1-y}Ln_y)O_{2-x}$, which is not possible for UO_2.

The sub-stoichiometry resulting from the reduction of Pu^{4+} to Pu^{3+} can also be found in the uranium-plutonium mixed oxide (MOX) [22–28]. The defective structure in hypo-stoichiometric $(U_{1-y}Pu_y)O_{2-x}$ is interpreted in terms of a clustering of the Pu^{3+} and oxygen vacancies. The Markin-McIver rule [22] proposed that the oxygen potential depends only on the average valence and not directly on the concentration of plutonium. However, the valence state of the lanthanide cation in $(U_{1-y}Ln_y)O_{2-x}$ system is intrinsic and always fixed at 3+. The oxygen potential depends directly on the substitution amount of the lanthanide cation.

Several researchers have measured the non-stoichiometry and electrical conductivity in the $(U,Ln^{3+})O_{2\pm x}$ system at various oxygen partial pressures and temperatures, and they have suggested various defect models based on those measurements [29–40]. The suggested defect models cover wide ranges of the substituted species, substitution amounts, and measuring temperatures so much so the oxygen defect models in a Ln^{3+} substituted UO_2 are difficult to integrate in a consistent manner. Nevertheless, it has been commonly stated that the defect is related to the oxygen interstitials in the hyper-stoichiometric region and it is related to the oxygen vacancies in the hypo-stoichiometric region. The hyper- and hypo-stoichiometry means the upper and lower deviations from the O/M ratio of 2.0, respectively. Thus the charge concentration should increase as the non-stoichiometry increases, regardless of the types of defects. The electrical conductivity vs. oxygen partial pressure curves of $(U,Ln^{3+})O_{2\pm x}$ should have a parabolic shape with a flat minimum at the O/M ratio of 2.0 as in the $Gd_2(Zr_xTi_{1-y}Ta_y)_2O_7$ system [41].

However, several electrical conductivity measurements of $(U,Ln^{3+})O_{2-x}$ in the hypo-stoichiometric region have shown somewhat opposite results. Matsui et al. found that the electrical conductivity of the hypo-stoichiometric $(U_{1-y}La_y)O_{2-x}$ slightly decreased with decreasing oxygen partial pressure [22]. Ohmichi et al. also found that the isothermal electrical conductivity of hypo-stoichiometric $(U_{1-y}Y_y)O_{2-x}$ decreased with an increase of the oxygen deficiency x [36].

Inconsistency can also be found in the hyper-stoichiometric region. The electrical conductivity is the product of the concentration and mobility of the charge carriers. The concentration of mobile charge carriers is proportional to the oxygen deviation from the stoichiometry, which is determined by the oxygen partial pressure. It is known that the hole mobility for the same type of oxygen defects is almost independent of the change in the oxygen partial pressure [29,40]. This implies that the α and β values in the $x \propto p_{O_2}^{1/\alpha}$ and $\sigma \propto p_{O_2}^{1/\beta}$ equations should be closely interrelated. However, in most cases of the $(U,Ln^{3+})O_{2\pm x}$ system, the two values are quite different from each other, and moreover, relations between them are not clearly explained as yet.

In this study, the electrical conductivity and non-stoichiometry, x, of $(U_{1-y}Gd_y)O_{2\pm x}$ $(y = 0.087, 0.169)$ were measured at various oxygen partial pressures at 1200 °C and 1300 °C. A new stoichiometry was proposed to explain in a congruent way the relationship between the electrical conductivity and the non-stoichiometry. The defect structure of $(U,Gd^{3+})O_{2\pm x}$ was deduced from both the electrical conductivity and non-stoichiometry change based on the new stoichiometric oxygen composition.

2. Experimental

Wet ball-milled powders of 6 wt% and 12 wt% Gd_2O_3-doped UO_2 were pressed into cylindrical pellets and sintered in H_2 at 1730 °C for 4 h. The sintered pellets were held at 1650 °C for 20 h in a gas mixture of CO_2 and H_2 ($CO_2/H_2 = 0.3$) for the purpose of chemical homogenization. The annealed sample pellets were cooled to room temperature in 3 vol.% CO_2 containing H_2. The formation of the single-phase solid solution was characterized by X-ray diffraction and EPMA area mapping. For the thermogravimetric studies, 1.5 g of the pellet samples were loaded into a TGA (Shimadzu, TG-50) and the isothermal weight changes according to the variation of the oxygen partial pressure were measured. The oxygen partial pressure was controlled by flowing various CO and CO_2 gas mixtures and monitored by an oxygen sensor. The electrical conductivity was measured by the conventional DC 4-probe method. Two Pt plates were attached to both ends of the cylindrical sample pellet, and two Pt wires in the vicinity of both ends. The constant currents were applied stepwise through the two Pt plates in the range from −40 mA to 40 mA with a 5 mA interval. The corresponding voltage drops between the two inner Pt-wire probes were measured.

3. Results and discussion

3.1. Dependence of the non-stoichiometry and electrical conductivity on the oxygen partial pressure

Fig. 1(a) displays the isothermal O/M ratio changes of $(U_{1-y}Gd_y)O_{2\pm x}$ $(y = 0.087, 0.169)$ as a function of the oxygen partial pressure measured at 1200 °C and 1300 °C. As the Gd contents or temperature increase, the O/M ratio shifts to a higher p_{O_2} region, and the p_{O_2} range showing a constant O/M ratio tends to become more narrow. $\log x$ vs. $\log p_{O_2}$ is plotted to obtain the value α in the $x \propto p_{O_2}^{1/\alpha}$ relation and are shown in Fig. 1(b). The exponent α is about 1 for the hyper-stoichiom-

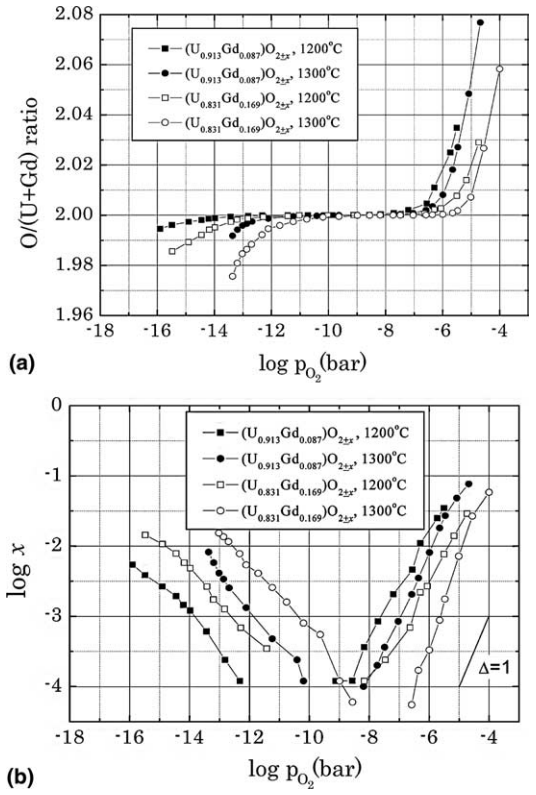

Fig. 1. (a) Dependence of the metal to oxygen ratio, O/(U + Gd), on the oxygen partial pressure of $(U_{1-y}Gd_y)O_{2\pm x}$. (b) Dependence of the oxygen non-stoichiometry, x, on the oxygen partial pressure of $(U_{1-y}Gd_y)O_{2\pm x}$.

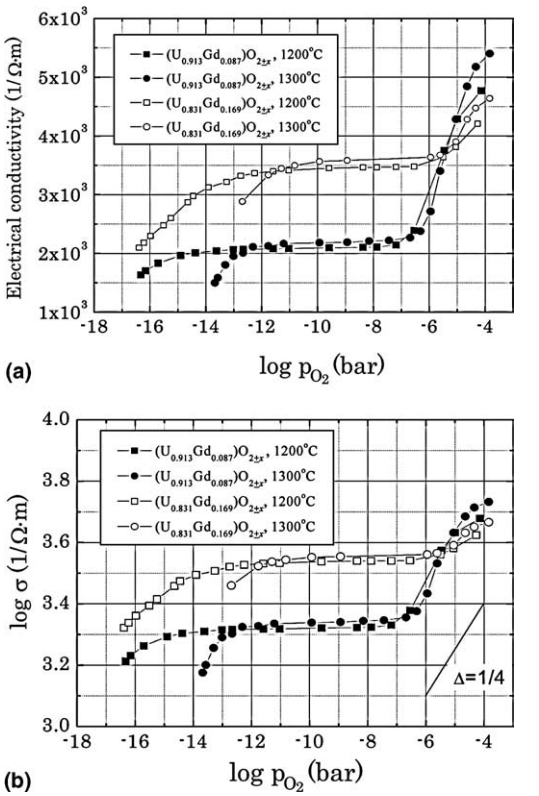

Fig. 2. (a) Dependence of the electrical conductivity, σ, on the oxygen partial pressure of $(U_{1-y}Gd_y)O_{2\pm x}$. (b) Plots of the $\log\sigma$ vs. $\log p_{O_2}$ of $(U_{1-y}Gd_y)O_{2\pm x}$.

etric region and about -2 for the hypo-stoichiometric region, respectively. These results agree well with other measurements [31].

Fig. 2(a) shows the isothermal electrical conductivity changes. The electrical conductivity curves show basically the same features as those of the O/M ratio; they are decreasing, remaining constant and then decreasing as the oxygen partial pressure decreases. It is interesting to note that the electrical conductivity continues to decrease even in the hypo-stoichiometric region. This result is in contrast to the commonly accepted defect model that the electrical conductivity should increase due to the creation of free electrons in the hypo-stoichiometric region.

Fig. 2(b) shows the plot of $\log\sigma$ vs. $\log p_{O_2}$. From the comparison of Fig. 1(b) and Fig. 2(b), we can see that the shape and the slopes of the two curves are totally different from each other in both the hypo-stoichiometric and hyper-stoichiometric regions. The dependence of the oxygen non-stoichiometry suggests that the oxygen vacancy type defect concentration increases with the decrease of p_{O_2} in the hypo-stoichiometric region. However, the electrical conductivity continues to decrease, suggesting that the defect in the hypo-stoichiometric region might not be an oxygen vacancy that can create free electrons. In the hyper-stoichiometric region, both the oxygen non-stoichiometry and electrical conductivity increase with increasing oxygen partial pressure. However, the slopes of the two curves are quite different from each other. The slope of the electrical conductivity curve of $(U_{0.913}Gd_{0.087})O_{2\pm x}$ is about 1/4. In the case of the $(U_{0.831}Gd_{0.169})O_{2\pm x}$ system, the slope is about 1/12. On the other hand, the slopes of the non-stoichiometry curves of $(U_{0.913}Gd_{0.087})O_{2\pm x}$ and $(U_{0.831}Gd_{0.169})O_{2\pm x}$ in a high p_{O_2} region show the value of 1. Similar differences between α and β are generally found in $(U,Ln^{3+})O_{2\pm x}$ systems [40]. But, any reasonable correlations between the two exponents have not been suggested as yet.

The charge neutrality condition of $[h^{\bullet}] = [Ln'_U] =$ constant is frequently introduced to interpret the flat electrical conductivity dependence in the intermediate oxygen partial pressure region of the $(U,Ln^{3+})O_{2\pm x}$ system [34,40]. The electrical conductivity is constant when the $[h^{\bullet}] = [Ln'_U] =$ constant condition

prevails. The defect model in the intermediate oxygen partial pressure region can be deduced only from the dependence of the oxygen non-stoichiometry on p_{O_2}.

3.2. A new definition of the stoichiometry in the $(U,Gd^{3+})O_{2\pm x}$ system

The stoichiometric O/M ratio of Gd_2O_3 doped UO_2 is usually defined as 2. The chemical formula of Gd_2O_3 doped UO_2 is generally denoted as

$$(U_{1-y}Gd_y)O_{2\pm x} \tag{1}$$

The non-stoichiometry x denotes the deviation from 2. The chemical formula of $(U_{1-y}Gd_y)O_2$ can be divided as

$$\left(U^{4+}_{1-2y}Gd^{3+}_{y}O^{2-}_{2-\frac{y}{2}}\right)\cdot\left(U^{5+}_{y}O^{2-}_{\frac{y}{2}}\right) \tag{2}$$

It implies that a negatively charged oxygen atom at an oxygen concentration of 2 compensates for the U^{5+} cation. The U^{5+} cation atoms can be reduced to U^{4+} cation atoms. Therefore, the fully reduced composition is described as

$$\left(U^{4+}_{1-y}Gd^{3+}_{y}\right)O_{2-\frac{y}{2}} \tag{3}$$

Lindemer and Sutton [21] have found that x of $\left(U^{4+}_{1-y}Gd^{3+}_{y}\right)O_{2-x}$ was converted very closely to $2.0-y/2$ as the oxygen potential was lowered when the substituted amount of Gd was not too high. Fujino et al. [42–44] have tried to explain the oxygen potential of the M^{3+} cation-substituted UO_2 system in terms of the configurational mixing of various kinds of cation complexes. According to their calculations, the oxygen potential of $\left(U_{1-y}Ln^{3+}_{y}\right)O_{2.0\pm x}$ was rapidly decreased at an oxygen composition of $2-y/2$ because the configurational entropy was diverged to an infinite value. The composition of the stoichiometric phase is not changed by the oxygen potential in a certain oxygen potential range. Therefore, Lindemer's experimental results and Fujino's computational results suggest that the phase having chemical composition of Eq. (3) could be a new stoichiometric phase in the Gd doped UO_2 system. Then, the oxygen deviation z from a new stoichiometry can be expressed as

$$\left(U^{4+}_{1-y-2z}U^{5+}_{2z}Gd^{3+}_{y}\right)O_{2-\frac{y}{2}+z} \tag{4}$$

The newly defined non-stoichiometry z and x in Eq. (1) has the following relation:

$$z = x + y/2. \tag{5}$$

Nakajima et al. [45] measured the oxygen potential of a hypo-stoichiometric $(U,Y)O_{2-x}$ solid solution using a mass spectrometer. They found that the oxygen potential of $U_{1-y}Y_yO_{2-y/2}$ was almost in agreement with that of pure urania having the same oxygen deficits ($UO_{2-y/2}$).

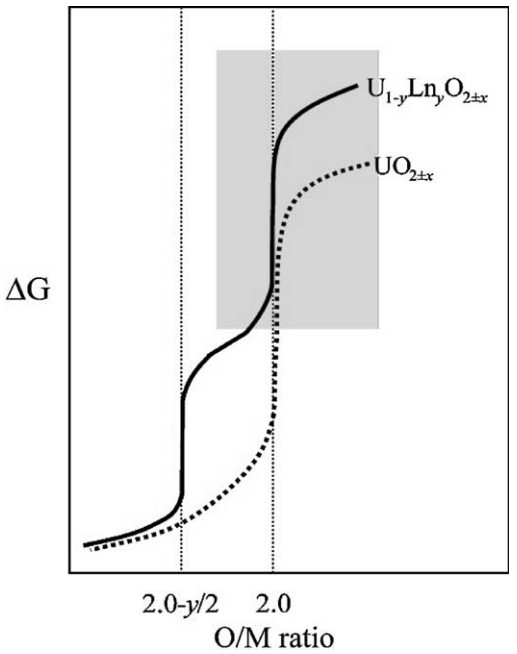

Fig. 3. Schematic representation of the Gibbs energy of oxygen on the composition in the $(U_{1-y}Ln_y)O_{2+x}$ solid solution together with that of UO_{2+x}. The dark area corresponds to the experimental range of this work.

This result might be controversial because the oxygen potentials of the solid solutions containing the trivalent M^{3+} ion are generally known to be more positive than those of pure urania. However, if we assume a new stoichiometric phase below the O/M ratio of 2, this result can be relatively well understood. Fig. 3 represents schematically the variation of the oxygen potential using the concepts of new and original stoichiometry in $U_{1-y}Ln_yO_{2\pm x}$ together with UO_{2+x}. At $x = y/2$, the oxygen potential of $U_{1-y}Y_yO_{2-y/2}$ might be decreased to such an extent that it is almost the same as that of $UO_{2-y/2}$. In addition, the configurational entropy, consequently the oxygen potential, of the two phases might be in accord with each other because each concentration of Y^{3+} and U^{4+} in $U_{1-y}Y_yO_{2-y/2}$ is the same as that of charged oxygen vacancies and U^{4+} in UO_{2-x}. The experimental data of Nakajima et al. [45] could also support that $U_{1-y}Y_yO_{2-y/2}$ is a stoichiometric composition.

The oxygen partial pressure dependence of the new non-stoichiometry z was recalculated according to Eq. (4). The non-stoichiometric dependence curves are plotted in Fig. 4, together with those of the conductivity. As shown in these figures, the recalculated non-stoichiometric dependence curves are in good agreement with those of the electrical conductivity. The recalculated non-stoichiometric dependence curves suggest that the defect type is always oxygen interstitial even below the O/M ratio of 2.0. We can also observe that the oxygen concen-

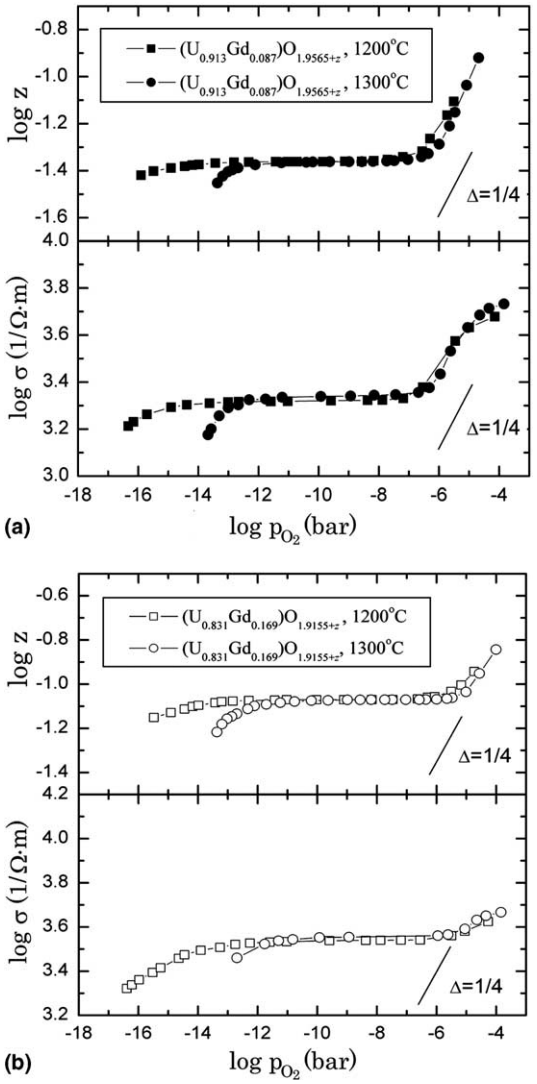

Fig. 4. Revised dependence of the oxygen non-stoichiometry, z, on the oxygen partial pressure together with the dependence of the electrical conductivity. The z is the oxygen non-stoichiometry in $(U_{1-y}Gd_y)O_{2-y/2+z}$: (a) $(U_{0.913}Gd_{0.087})O_{2-y/2+z}$ and (b) $(U_{0.831}Gd_{0.169})O_{2-y/2+z}$.

tration does not change in the intermediate p_{O_2} region, and that the slopes of the curves in a high p_{O_2} region are almost the same as those of the electrical conductivity curves. These findings are quite different from those of Fig. 1(b) but almost identical to those of the electrical conductivity dependence curves in Fig. 2(b).

When the new definition of a reference stoichiometry of Eq. (3) is applied to the MOX system, the situation is somewhat different. According to the oxygen potential calculation of Schmitz [24], the oxygen potential of $(U_{1-y}Pu_y)O_{2-x}$ is also abruptly diminished at $x = y/2$. However, Fujino et al. [46] show that the electrical conductivity of $(U_{0.1}Pu_{0.9})O_{2-x}$ is increased with a decrease of oxygen partial pressure at a low oxygen partial pressures. This fact confirms that the defect concentration is increased as the O/M ratio deviates more from 2, and the defect type of the hypo-stoichiometric MOX is an oxygen vacancy, i.e. free electron. As aforementioned, a new kind of cation having a different valence state, Pu^{3+}, is created in the hypo-stoichiometric region of the MOX system, and its concentration is increased with decreasing oxygen partial pressure. Whereas, in the $(U_{1-y}Ln_y)O_{2\pm x}$ system, any new kind of cation is not created in the hypo-stoichiometric region. Only the concentration of the existing U^{5+} is diminished with an oxygen partial pressure decrease until all the U^{5+} cations are reduced to U^{4+} cations. The decrease of the electrical conductivity in a low partial pressure region verifies the diminution of the defect concentration, i.e. holes, in the hypo-stoichiometric region with decreasing oxygen partial pressure. The difference of defect type between $(U,Pu)O_{2-x}$ and $(U,Ln)O_{2-x}$ suggests that, when we choose the reference stoichiometry for interpreting the defect structure, it should be considered whether a new type of cation having a different valence state appears or not across the stoichiometric composition.

3.3. Defect structure of the $(U,Gd^{3+})O_{2\pm x}$ system

By applying the new stoichiometry of Eq. (4), the slope of the non-stoichiometry dependence curves of Fig. 1(a) was largely changed in Fig. 4. The most of suggested defect structures in the U_{1-y} $Gd_yO_{2-y/2+z}$ system were analyzed with the slopes in Fig. 1(b). Therefore the defect structure needs to be revised according to the slopes in Fig. 4.

The structural determination of the defect structure in the hypo-stoichiometric $(U,Ln^{3+})O_{2-x}$ system has not been systematically carried out as yet. However, the oxygen vacancy cluster models including a dopant have been suggested [25,26,38]. These defect structure models might be applicable by changing the oxygen vacancies to oxygen interstitials. The dependence curves measured at 1200 °C show smoothly changing curvatures in a low p_{O_2} region, so it is difficult to clearly determine the slope. However, the α or values are determined to be 4–5 for both the solid solutions from the dependence curves measured at 1300 °C. This value implies that the incorporated oxygen interstitials are not simply associated but form defect clusters [31]. Particularly, the very similar slope to that in the high oxygen partial pressure region suggests that the defect structure in the low oxygen partial region may be similar to that in the high oxygen partial pressure region.

According to Eq. (2), the charge neutrality condition in the intermediate oxygen partial pressure region can be expressed as

$$[h^{\bullet}] = 2[O_i''] = 2z = [Gd] = \text{constant}. \quad (6)$$

The hole mobility in the $(U,Ln^{3+})O_{2\pm x}$ system is known to decrease with an increase of the Ln^{3+} concentration due to the decrease of the available hole hopping sites [29,47]. Eq. (6) also suggests the possibility that the hole concentration might be non-linearly proportional to the [Gd] concentration when the cation clustering occurs especially in a high [Gd] containing solid solution.

The most frequently adopted defect cluster for hyper-stoichiometric system is either the $(2V_O 2O_i^a 2O_i^b)^{m'}$ or $(2V_O O_i^a 2O_i^b)^{n'}$ cluster which involves two kinds of interstitial oxygens and vacancies. The oxygen partial pressure dependence of the non-stoichiometry z is obtained as $z \propto p_{O_2}^{1/(m+1)}$ for the $(2V_O 2O_i^a 2O_i^b)^{m'}$ cluster and $z \propto p_{O_2}^{1/2(n+1)}$ for the $(2V_O O_i^a 2O_i^b)^{n'}$ cluster. The slope for the $(U_{0.913}Gd_{0.087})O_{2-2/y+z}$ solid solution in a high p_{O_2} is about 1/4. It can be explained by both the $(2O_i^a 2V_O 2O_i^b)^{3'}$ or $(O_i^a 2V_O 2O_i^b)'$ defect cluster model. In the case of the $(U_{0.831}Gd_{0.169})O_{2-2/y+z}$ solid solution, the slope is about 1/5. In this case, the $(2O_i^a 2V_O 2O_i^b)^{4'}$ defect cluster model can be suggested. If we assume that the major defect structure does not change and only its valence state varies with the Gd contents, the $(2O_i^a 2V_O 2O_i^b)$ defect is more plausible for the defect model at high p_{O_2}.

There is a noticeable difference between the non-stoichiometry and electrical dependence curves in a high p_{O_2} region. The conductivity curves depart from the linear dependence near or above $p_{O_2} \approx 10^{-5}$ bar. From Fig. 4(a) and (b), we can found that the oxygen partial pressure at the inflection is almost independent of the Gd concentration. In addition, the corresponding new oxygen non-stoichiometry z at the inflection is also independent of the Gd contents and has a value of about 0.1. The observed oxygen partial pressure at an inflection point and a corresponding oxygen non-stoichiometry z are found to be almost the same as those observed in the UO_2 base fluorites such as UO_{2+x}, $(U_{1-y}Y_y)O_{2+x}$ [29] and $(U_{1-y}Er_y)O_{2+x}$ [40], when the experimental data of these systems are reanalyzed using our new stoichiometry, i.e., UO_{2+z}, $(U_{1-y}Y_y)O_{2-y/2+z}$ and $(U_{1-y}Er_y)\ O_{2-y/2+z}$. This implies that the electrical conductivity curves of $(U,Ln^{3+})O_{2-y/2+z}$ are inflected when the oxygen non-stoichiometry z exceeds 0.1 regardless of the amount or species of the doped cation. The oxygen non-stoichiometry z can be converted to the U^{4+} fraction ($f_{U^{4+}}$) from the total cations by using Eq. (4). The electrical conductivity departs from the linear dependence when the fraction of U^{4+} per total cations becomes smaller than about 0.8. This slope change in the electrical conductivity curves above $p_{O_2} \approx 10^{-5}$ bar may be associated with a suppression of the charge mobility since the non-stoichiometry, i.e., charge concentration, linearly increases even above $p_{O_2} \approx 10^{-5}$ bar.

A relationship between the oxygen partial pressure and hole concentration makes it possible to calculate the mobility of the hole using the following equation:

$$\mu_h = \frac{\sigma}{q \cdot C_h}. \quad (7)$$

The q is the elementary charge and C_h is the hole concentration. This concentration, and the oxygen non-stoichiometry, z, per fluorite unit cell are related as follows:

$$C_h = A \cdot \frac{4 \cdot [z]}{a^3}, \quad (8)$$

where a is a lattice parameter. The defect type and its valence state determine the constant A. From Eqs. (7) and (8), the mobility of μ_h is given in terms of the electrical conductivity and non-stoichiometry as follows:

$$\mu_h = \frac{\sigma \cdot a^3}{4A \cdot q \cdot [z]}. \quad (9)$$

From Eq. (6), the A value in the intermediate oxygen partial pressure region for both solid solutions is 2. The significance of A in a low and high oxygen partial pressure region is not clear at present, but if we tentatively

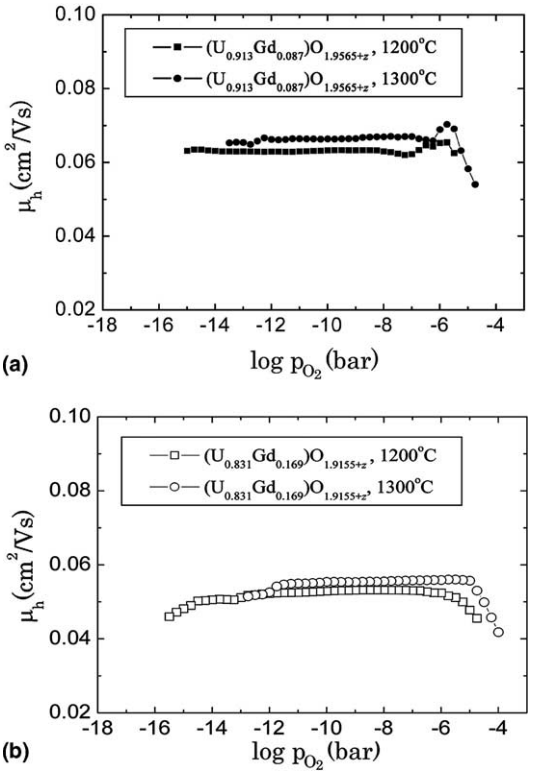

Fig. 5. Hole mobility of $(U_{1-y}Gd_y)O_{2-y/2+z}$ as a function of the oxygen partial pressure: (a) $(U_{0.913}Gd_{0.087})O_{2-y/2+z}$ and (b) $(U_{0.831}Gd_{0.169})O_{2-y/2+z}$.

assume that the incorporated oxygen is fully ionized regardless of the defect type, then A is 2 in the whole oxygen partial pressure range for both solid solutions.

Fig. 5 shows the calculated hole mobility for both solid solutions based on the assumption that the incorporated oxygens are fully ionized. The calculated mobility is in agreement with the other trivalent cation-doped UO_2 systems [29,40]. The hole mobility of the $(U_{0.831}Gd_{0.169})O_{2-y/2+x}$ system does not change with oxygen partial pressures below $p_{O_2} \approx 10^{-5}$ bar. This reveals that the incorporated oxygen atoms in the solid solution were fully ionized regardless of the oxygen defect structure because the mobility of the same type charge carrier is known to be constant. However, in the $(U_{0.913}Gd_{0.087})O_{2-y/2+x}$ system, the hole mobility increases in a high p_{O_2} region between 10^{-7} bar and 10^{-5} bar. The increase of the hole mobility may be due to the difference in the charge state of incorporated oxygen. It might be worth noting that the hole mobility of both solid solutions decreased linearly at high oxygen partial pressure above $p_{O_2} \approx 10^{-5}$ bar. In a small polaron hopping mechanism [48], the hole mobility is directly proportional to the fraction of the unoccupied site available for a carrier occupancy. The decrease of the hole mobility in a high oxygen partial pressure above $p_{O_2} \approx 10^{-5}$ bar might be ascribed to the diminution of the unoccupied site available for a carrier occupancy.

4. Conclusion

The isothermal electrical conductivity of the $(U_{0.913}Gd_{0.087})O_{2\pm x}$ and $(U_{0.831}Gd_{0.169})O_{2\pm x}$ systems decreased with decreasing oxygen partial pressure not only in the hyper-stoichiometric but also in the hypo-stoichiometric region. This result cannot be understood by the commonly accepted defect model where oxygen vacancy type defects prevail in the hypo-stoichiometric region and thus the electrical conductivity should increase with decreasing oxygen partial pressure by means of the formation of the free electrons.

Based on the literature where the $(U_{1-y}Ln_y)O_{2-y/2}$ composition is constant in a certain range of the oxygen partial pressure, $(U_{1-y}Gd_y)O_{2-y/2}$ is defined as a new stoichiometric phase. The dependence of the new oxygen non-stoichiometry z in $(U_{1-y}Gd_y)O_{2-y/2+z}$ on the oxygen partial pressure suggests that the defect type is an oxygen interstitial even below the oxygen composition of 2, just as the electrical conductivity curve does. In addition, the oxygen composition maintains constant in the intermediate p_{O_2} region, and the slopes of the curves in a high p_{O_2} region are almost consistent with those of the electrical conductivity curves.

The hole mobility of both solid solutions in the total measured oxygen partial pressure region was calculated using the correlation between the oxygen non-stoichiometry and the electrical conductivity. The hole mobility was found to remain almost unchanged, regardless of the defect cluster type, with the oxygen partial pressure change as far as the ionization state of the defective oxygen atom remains constant. However, the hole mobility of both solid solutions decreases linearly with the oxygen partial pressure increase when it exceeds $p_{O_2} \approx 10^{-5}$ bar.

Acknowledgments

The authors express their appreciation to Dr Hj. Matzke of Institute of Transuranium Elements (ITU), Karlsruhe for valuable discussions. This study has been carried out under the Nuclear R&D Program by MOST (Ministry of Science and Technology) in Korea.

References

[1] B.T.M. Willis, Proc. Brit. Ceram. Soc. 1 (1964) 9.
[2] H. Blank, C. Ronchi, Acta Crystallogr. A 34 (1968) 657.
[3] B.T.M. Willis, Acta Crystallogr. A 34 (1978) 88.
[4] T.B. Lindemer, T.M. Besmann, J. Nucl. Mater. 130 (1985) 473.
[5] D.J.M. Bevan, I.E. Grey, B.T.M. Willis, J. Solid State Chem. 61 (1986) 1.
[6] G.C. Allen, P.A. Tempest, Proc. R. Soc. Lond. A 406 (1986) 325.
[7] A.D. Murray, B.T.M. Willis, J. Solid State Chem. 84 (1990) 52.
[8] M. Hofmann, S. Hull, G.J. McIntyre, C.C. Wilson, J. Phys.: Condens. Matter 9 (1997) 845.
[9] L. Nowicki, F. Garrido, A. Turos, L. Thomé, J. Phys. Chem. Solids 61 (2000) 1789.
[10] F. Garrido, R.M. Ibberson, L. Nowicki, B.T.M. Willis, J. Nucl. Mater. 322 (2003) 87.
[11] O.T. Sørensen, in: Nonstoichiometric Oxides, Academic Press, 1981, p. 1.
[12] H.M. Lee, J. Nucl. Mater. 48 (1973) 107.
[13] T. Matsui, K. Naito, J. Nucl. Mater. 132 (1985) 212.
[14] S.H. Kang, J.H. Lee, H.I. Yoo, H.S. Kim, Y.W. Lee, J. Nucl. Mater. 277 (2000) 339.
[15] T. Yamashita, K. Ohuchi, T. Tsuji, T. Kato, M. Ochida, M. Iwashita, J. Alloys Compd. 271 (1998) 400.
[16] H. Bairiot, P. Deramaix, C. Vandenburg, in: Improved Utilization of Water Reactor Fuel, with Special Emphasis on Extended Burnups and Plutonium Recycling, Proceedings of the Special IAEA meeting, Report conference 8405285, 1984, p. 86.
[17] H. Assmann, J.P. Robin, in: Guidebook on Quality Control of Mixed Oxides and Gadolinium Bearing Fuels for Light Water Reactors, IAEA-TECDOC-584, IAEA, Vienna, 1983, p. 51.
[18] K.W. Song, K.S. Kim, H.S. Yoo, Y.H. Jung, J. Korean Nucl. Soc. 30 (1998) 128.
[19] K.W. Song, K.S. Kim, J.H. Yang, K.W. Kang, Y.H. Jung, J. Nucl. Mater. 277 (2001) 92.

[20] T.B. Lindemer, J. Brynestad, J. Am. Ceram. Soc. 69 (1986) 867.
[21] T.B. Lindemer, A.L. Sutton Jr., J. Am. Ceram. Soc. 71 (1989) 553.
[22] T.L. Markin, E.J. McIver, in: Proceedings of the 3rd International Conference on Plutonium, Institute of Metals, London, 1965, p. 845.
[23] R.E. Woodley, J. Nucl. Mater. 96 (1981) 5.
[24] F. Schmitz, J. Nucl. Mater. 47 (1973) 366.
[25] C.R.A. Catlow, J. Nucl. Mater. 67 (1977) 236.
[26] J.H. Harding, R. Pandey, J. Nucl. Mater. 125 (1984) 125.
[27] D. Glasser-Leme, Hj. Matzke, Solid State Ionics 12 (1984) 217.
[28] Hj. Matzke, in: Advances in Ceramics, Fission Products Behavior in Ceramic Oxide Fuel, vol. 17, Am. Ceram. Soc., Westville, Columbus, OH, 1986, p. 1.
[29] N.J. Dudney, R.L. Coble, H.L. Tuller, J. Am. Ceram. Soc. 64 (1981) 627.
[30] K. Une, M. Oguma, J. Nucl. Mater. 110 (1982) 215.
[31] K. Une, M. Oguma, J. Nucl. Mater. 115 (1983) 84.
[32] K. Une, M. Oguma, J. Nucl. Mater. 118 (1983) 189.
[33] K. Une, M. Oguma, J. Nucl. Mater. 131 (1985) 88.
[34] T. Matsui, K. Naito, J. Nucl. Mater. 138 (1986) 19.
[35] T. Matsui, K. Nato, J. Nucl. Mater. 151 (1987) 86.
[36] T. Ohmichi, H. Takeshita, S. Fukushima, A. Maeda, J. Nucl. Mater. 151 (1987) 90.
[37] T. Fujino, J. Nucl. Mater. 154 (1988) 14.
[38] K. Park, D.R. Olander, J. Nucl. Mater. 187 (1992) 89.
[39] H.S. Kim, Y.K. Yoon, Y.W. Lee, J. Nucl. Mater. 226 (1995) 206.
[40] S.H. Kang, J.D. Yi, H.-I. Yoo, S.H. Kim, Y.W. Lee, J. Phys. Chem. Solids 63 (2002) 773.
[41] H.L. Tuller, Solid State Ionics 94 (1997) 63.
[42] T. Fujino, N. Sato, J. Nucl. Mater. 189 (1992) 103.
[43] T. Fujino, N. Sato, K. Yamata, J. Nucl. Mater. 223 (1995) 6.
[44] T. Fujino, N. Sato, J. Nucl. Mater. 282 (2000) 232.
[45] K. Nakajima, T. Ohmichi, Y. Arai, J. Nucl. Mater. 304 (2002) 176.
[46] T. Fujino, T. Yamashita, K. Ouchi, K. Naito, T. Tsuji, J. Nucl. Mater. 202 (1993) 154.
[47] K. Hagemark, M. Broli, J. Inorg. Nucl. Chem. 28 (1966) 2837.
[48] H.L. Tuller, A.S. Nowick, J. Phys. Chem. Solids 38 (1977) 859.